J BONE ONCOL 49 (2024) 100646

Contents lists available at ScienceDirect

Journal of Bone Oncology

journal homepage: www.elsevier.com/locate/jbo

# Clinical decision-making in bone cancer care management and forecast of ICU needs based on computed tomography

Huan Xu [a,*], Qunfang Zhao [b], Xiaoyan Miao [c], Lijun Zhu [d], Junping Wang [a]

[a] Department of Hospital Infection Management, The First People's Hospital of Fuyang, Hangzhou 311400, China
[b] Department of Renal and Endocrinology, The First People's Hospital of Fuyang, Hangzhou 311400, China
[c] Radiation Oncology Center, The First People's Hospital of Fuyang, Hangzhou 311400, China
[d] Department of Critical Care Medicine, The First People's Hospital of Fuyang, Hangzhou 311400, China

## HIGHLIGHTS

- Evaluated CT for bone cancer diagnosis and management during limited histopathological testing access.
- Conducted retrospective analysis of 60 patients with bone cancer.
- Determined likelihood of bone cancer based on CT study adhered to established oncological guidelines.
- Findings highlight importance of CT in diagnosing and managing bone cancer.

## ARTICLE INFO

*Keywords:*
Bone cancer
Computed tomography
Osteolytic lesions
CT severity score
Histopathological testing
ICU admissions

## ABSTRACT

*Objective:* This study aimed to evaluate the role of computed tomography (CT) imaging in the diagnosis and management of bone cancer during periods of limited access to histopathological testing. We aimed to determine the correlation between CT severity levels and subsequent patient management and care decisions, adhering to established oncological CT reporting guidelines.
*Methodology:* A retrospective analysis was conducted on 60 symptomatic patients from January 2021 to January 2024. The cohort included patients aged between 50 and 86 years, with a mean age of 68 years, and 75 % were male. All patients had their bone cancer diagnosis confirmed through histopathological examination, and CT imaging was used as the reference method. The analysis involved assessing the correlation between CT severity scores and patient management, including ICU admissions.
*Results:* The study found that CT imaging demonstrated a sensitivity of 92.6% in diagnosing bone cancer, with accuracy increasing to 97.6% in cases with high-probability CT characteristics. CT specificity also showed a consistent rise. Osteolytic lesions were the predominant finding, detected in 85.9% of cases. Among these, 88% exhibited engagement across multiple skeletal regions, 92.8% showed bilateral distribution, and 92.8% presented with peripheral involvement. In ICU patients, bone consolidation was observed in 81.5% of cases and was predominant in 66.7% of the ICU cohort. Additionally, ICU patients had significantly higher CT severity scores, with scores exceeding 14 being notably prevalent.
*Conclusions:* During the management period of bone cancer at our hospital, characteristic features on CT imaging facilitated swift and sensitive investigation. Two distinct CT phenotypes, associated with the primary osteolytic phenotype and severity score, emerged as valuable indicators for assessing the severity of the disease, particularly during ICU care. These findings highlight the diverse manifestations and severity levels encountered in bone cancer patients and underscore the importance of CT imaging in their diagnosis and management.

## 1. Introduction

Bone cancer, a member of the broader group of musculoskeletal neoplasms, can lead to severe morbidity and mortality. Primary bone cancers, such as osteosarcoma [30–33], Ewing sarcoma, and chondrosarcoma [27], represent a critical area of oncology due to their

* Corresponding author.
*E-mail address:* xuhuan@ocibe.com (H. Xu).

https://doi.org/10.1016/j.jbo.2024.100646
Received 24 June 2024; Received in revised form 23 October 2024; Accepted 24 October 2024
Available online 2 November 2024

aggressive nature and complex treatment requirements [1,2]. These malignancies often present with varying symptoms, including localized pain, swelling, and reduced mobility, depending on the tumor's location and size. The pathogenesis of bone cancer involves complex genetic and molecular pathways, with particular attention to mutations and aberrant signaling mechanisms [3]. The impact of bone cancer is extensive, affecting patients' quality of life and requiring multidisciplinary approaches for management, including surgery, chemotherapy [34,35], and radiation therapy. Recent advancements in imaging techniques, particularly high-resolution CT, have significantly improved diagnostic accuracy and treatment planning [4]. The global burden of bone cancer remains substantial, with thousands of new cases diagnosed [29] annually, underscoring the need for continued research and improved therapeutic strategies [5,6]. The repercussions of bone cancer extend beyond the clinical sphere, affecting socioeconomic aspects such as healthcare costs and patients' ability to work, thereby imposing economic strains on families and healthcare systems. Continued efforts in public health, early diagnosis, and innovative treatments are crucial to mitigate the impact of this challenging disease [7].

Given the high specificity of histopathological examination for diagnosing bone cancer, it is commonly regarded as the gold standard. However, this method has limitations, including invasiveness, high costs, and potential delays in obtaining results [8]. Studies have shown that computed tomography (CT) can be highly effective in detecting bone malignancies, with sensitivity rates ranging from 60 % to 98 % and specificity from 25 % to 53 %. Histopathological sensitivity ranges from 42 % to 71 %, and results may vary over time [9]. Recent research has underscored the significance of CT imaging in diagnosing bone cancer. CT scans facilitate the assessment of tumor severity, monitoring disease progression, evaluating treatment efficacy, and categorizing various imaging characteristics and phenotypes based [37] on observed features [8–10]. This study aimed to evaluate the reliability of CT scans in diagnosing bone cancer by comparing their accuracy with histopathological results, following established oncological guidelines for CT interpretation. Furthermore, the study sought to establish a relationship between CT severity scores and the likelihood of requiring intensive care, as well as to identify specific imaging features and severity indicators associated with positive bone cancer cases. The application of radiomics and deep learning in predicting bone metastasis represents a significant advancement in the field of bone oncology [9–12]. These technologies offer a promising avenue for early detection and personalized treatment planning, ultimately improving patient outcomes and quality of life. This study aims to utilize radiomics and deep learning to predict the risk of bone metastasis based on CT scans of bone cancer [14], highlighting its important clinical significance. Incorporating the predictive capabilities of the deep learning model into clinical workflows [17] has the potential to significantly enhance the management of bone cancer patients at risk of bone metastasis. Early identification of high-risk patients can facilitate timely interventions, potentially improving prognosis and quality of life. Additionally, the model can aid in personalizing treatment plans by providing insights into individual risk profiles, thereby optimizing therapeutic strategies. Efficient risk stratification also allows for better allocation of healthcare resources, ensuring that patients who are most likely to benefit from intensive monitoring and treatment receive the necessary attention.

## 2. Methodology

This retrospective study, conducted at a single tertiary center, examines a cohort of 60 patients potentially affected by primary bone cancer between January 2021 to January 2024. The study focused on patients who underwent high-resolution bone CT scans without intravenous contrast. CT imaging utilized low kVp and low mAs settings to reduce radiation exposure while ensuring diagnostic efficacy. Ethical approval was granted by the institutional ethics committee, which waived the need for written informed consent given the study's retrospective design.

### 2.1. Inclusion criteria for patients suspected of bone cancer

All patients presenting to the emergency room (ER) or outpatient clinic with clinical symptoms suggestive of bone cancer were included. Symptoms considered included persistent bone pain, swelling, fractures without significant trauma, fatigue, weight loss, and unexplained anemia. These patients underwent non-contrast imaging studies such as MRI, CT, or X-ray and laboratory investigations, including biopsy and relevant blood tests. Additionally, patients with a history of malignancy or genetic predisposition to bone cancers were included.

### 2.2. Exclusion criteria for bone cancer study Participants

Patients were excluded if they were unable to participate in the management plan. Those who did not have access to essential diagnostic testing like biopsy or imaging were also excluded. Individuals whose imaging results were affected by significant artifacts or poor quality were not considered for the study. Furthermore, patients admitted to the intensive care unit (ICU) for medical conditions unrelated to bone cancer were excluded from the study.

### 2.3. Comprehensive computed tomography (CT) imaging Methodology for bone cancer diagnosis and management

For the procedure, America, GE, 590RT, 16-slice CT scanner were used. The hospital's oncology unit protocols were strictly followed during the imaging process to ensure accurate and safe diagnostic outcomes. There were no special preparations required for the patients undergoing CT scanning. Patients were positioned supine with their arms lifted above their heads to avoid artifacts. The imaging process employed a 512 × 512 matrix with a slice thickness of 1.25 mm and an interval of 0.625 mm. The tube speed was set at 35 mm per revolution, with a rotation time of 0.5 s, as per calibration. The CT scan operator minimized radiation exposure by adjusting the kVp and mAs settings to the lowest achievable values. Image processing and interpretation involved transferring the images to a workstation for the review of axial slices and multi-planar reformation. Two experienced radiologists, each with a minimum of three years of post-fellowship expertise and specializing in musculoskeletal imaging, meticulously examined the images. To reduce inter-observer variability, any disagreements between their interpretations were settled by consensus. The radiologists were blinded to both the study objectives and the clinical details of the patients. Documented imaging results included the characterization of bone lesions, evaluation of tumor extent, and assessment of associated features such as cortical destruction and periosteal reaction. Among the documented imaging results were:

- The presence or absence of osteolytic and osteoblastic lesions was identified by noting several characteristics, including the lesions' shape (irregular, well-defined, sclerotic, or lytic), location (epiphyseal, metaphyseal, or diaphyseal; axial or appendicular skeleton; and unilateral or bilateral involvement), and whether they were singular or multifocal (affecting multiple sites).
- Additional features such as periosteal reaction, cortical destruction, soft tissue mass, pathological fractures, matrix mineralization, and the presence of skip lesions were also evaluated.
- Reporting focused on which CT pattern—osteolytic, osteoblastic, or mixed—predominated in each instance.

CT probability evaluation: To determine the likelihood of bone cancer [28], the study adhered to established oncological guidelines. Classifications of high, intermediate, low, or negative probability were used to evaluate the CT scans, aligning with the typical categorizations of negative, benign, uncertain, and malignant. [9][43].

Evaluation of CT scan severity: We retrospectively assessed the severity of CT scans in cases of identified bone cancer. Each affected bone was divided into three zones: proximal, middle, and distal. The extent of involvement in each zone was graded as follows: 1 point for less than 25 % involvement, 2 points for 25–50 % involvement, 3 points for 50–75 % involvement, and 4 points for more than 75 % involvement. For all zones, a maximum score of 24 could be obtained. We compared the CT severity score with the treatment decisions made for each patient.

#### *2.3.1. Biopsy Procedures and clinical Decision-Making in bone cancer management*

Both incisional and excisional biopsies were performed on each subject as needed to obtain representative tissue samples. This could be done up to three times if the initial results were considered insufficient or inconclusive, despite the subjects meeting conventional high-likelihood criteria based on imaging and clinical assessment. Data on clinical decisions made during the evaluation were collected, including determinations regarding patients' need for surgical intervention, chemotherapy, radiation therapy, or palliative care. The decisions made by the oncology team adhered to hospital protocols for managing bone cancer, considering factors such as symptoms, biopsy results, tumor size, metastasis, and the presence of risk factors for disease progression. [15].

#### *2.3.2. Sample size determination for achieving 70 % sensitivity in CT detection of bone cancer*

Using the PSAA-11 software and the methods described by Simpson et al., it was determined that a sample size of at least 60 patients is necessary to achieve a sensitivity of 70 % for CT detection of bone cancer, given an estimated 50 % of patients testing positive via histo-pathological examination. With this sample size, the significance level (α-error) is set at 0.05, and 80 % statistical power is guaranteed.

#### *2.3.3. Data analysis and statistical methodology using IBM SPSS statistics software*

IBM SPSS Statistics software version 22.0 (IBM Corp., Chicago, USA, 2013) was used for the analysis of the collected data. Quantitative data underwent analysis through descriptive statistics, encompassing measures such as minimum, maximum, mean, and standard deviation (SD) for normally distributed data. The analysis of qualitative data included calculating the frequency and proportion of occurrences. The ANOVA test was used to compare more than two independent groups with normally distributed data, followed by the post hoc Bonferroni test. The Shapiro-Wilk test was applied to assess the normality of the data. The independent *t*-test was used to compare two independent groups with normally distributed data. For qualitative data, Fisher's exact test and the chi-square test were used to assess differences between proportions, followed by the post hoc Bonferroni test. The performance of various tests was evaluated using ROC curve analysis to distinguish between different groups. Statistical significance was set at $P < 0.005$.

## 3. Results

A retrospective analysis was conducted on a cohort of 60 patients presenting with clinical suspicion of bone cancer. The mean age of the patients ranged from 50 to 86 years, with a standard deviation of 68 years (Fig. 1). In the entire patient cohort, males accounted for 75 % of the population; among those testing positive for bone cancer, the male-to-female ratio was 1.6 (Table 1). The time interval between the initial clinical symptoms and the CT scan ranged from two to seven days.

In 2021, a cohort of 26 patients with suspected bone cancer was studied, characterized by an unequal gender distribution and an average age of 68.1 years, ranging from 54 to 85 years. In 2022, a cohort of 17 patients was studied, characterized by an unequal gender distribution of 13:4, and an average age of 66.4 years, ranging from 50 to 83 years. By 2023, the cohort decreased to 16 patients, with a higher proportion of males, resulting in a slight increase in the average age to 69.1 years. By

**Table 1**
Patients Range with yearly effect.

| Year | Total Patients | Male | Female | Age Range | Mean Age |
|---|---|---|---|---|---|
| 2021 | 26 | 19 | 7 | 54–85 | 68.1 |
| 2022 | 17 | 13 | 4 | 50–83 | 66.4 |
| 2023 | 16 | 12 | 4 | 53–86 | 69.1 |
| 2024 | 1 | 1 | 0 | 74 | 74 |
| Total/Avg | 60 | 45 | 15 | 50–86 | 68 |

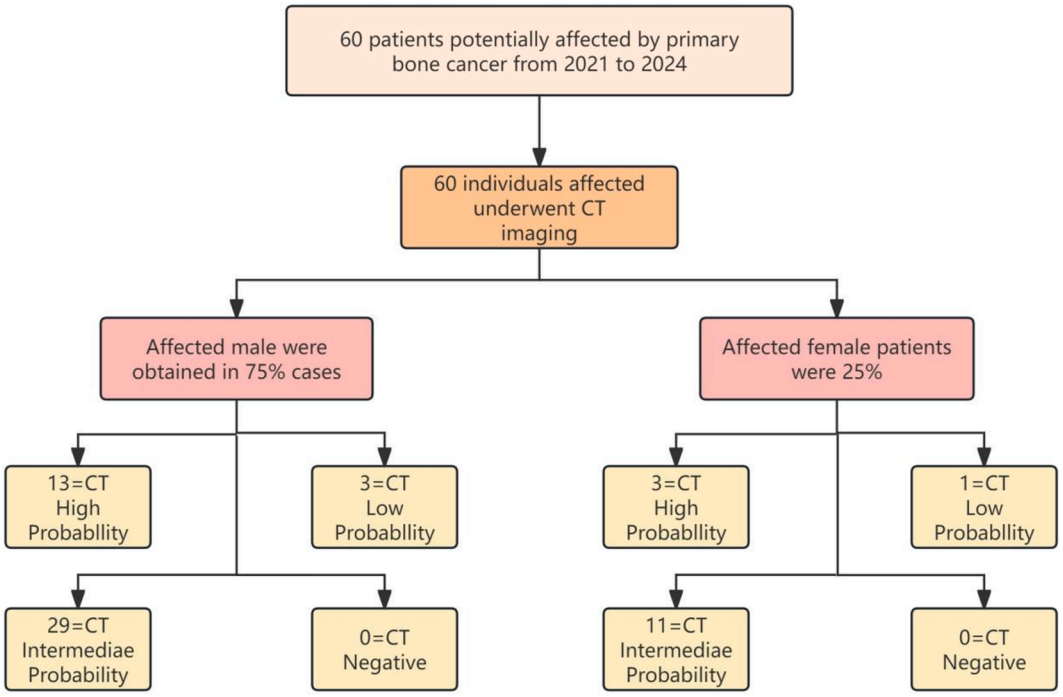


**Fig. 1.** The flow chart detailing patient progress within the nursing study environment.

2024, we only have one male and one female patient in our study. Over the four-year period, a total of 60 patients were included in the study, predominantly male, with an average age of 68 years, ranging from 50 to 86 years. This retrospective analysis aimed to assess demographic trends and characteristics among patients diagnosed with bone cancer, providing insights into age and gender distribution over the study period.

### *3.1. Comparing CT and histopathology in assessing treatment response for bone cancer*

This clinical study involved 60 patients undergoing computed tomography (CT) imaging before and after treatment [42]. The cohort comprised 45 males and 15 females, with ages ranging from 50 to 86 years and a mean age of 68 years. The study was conducted from January 2021 to January 2024 to assess treatment efficacy through CT imaging assessments. Lesions were delineated using red circles on the provided CT images, facilitating a comprehensive analysis of treatment response. These findings provide critical insights into optimizing therapeutic strategies for managing bone cancer, guiding future research and clinical practice. Further results are detailed in Figs. 2 and 3.

In this study, CT imaging was used to analyze a cohort of patients with Giant Cell Tumor of Bone (GCTB) to assess the prevalence and characteristics of identified abnormalities. The cohort consisted of individuals aged 50 to 86 years, with a mean age of 68 years, and included 45 males and 15 females. The study spanned from December 2022 to June 2023, during which patients underwent CT scans before and after treatment to evaluate treatment response. Abnormalities detected on CT scans were meticulously recorded, particularly focusing on characteristics such as GCTB and consolidation, as detailed in Table 2. Among positive cases, GCTB was observed in 85.9 % of instances, predominantly peripheral, multilobar, and bilateral as depicted in Fig. 2. Round forms accounted for 55.5 % of GCTB patterns, while the crazy-paving pattern was identified in 45.3 % of cases. Consolidation, seen in 28.8 % of positive cases, often exhibited subsegmental or segmental patterns, with 15.3 % showing clear consolidation exceeding GCTB.

The study identified two dominant CT phenotypes based on these features: one characterized by dominant GCTB and another by dominant consolidations (Figs. us. 2 and 3). Differences in consolidation and pleural effusion were noted between patient groups requiring different management strategies. Specifically, 44 ICU admissions were associated with a consolidation pattern on CT, with consolidation being more prevalent than GCTB in 66.7 % of ICU patients. Additionally, 23 out of 38 patients with pleural effusion on CT scans required ICU hospitalization (Table 2). These findings highlight the utility of CT imaging in assessing treatment response and guiding management decisions in GCTB. Giant Cell Tumor of Bone (GCTB) was the most common feature observed in the imaging patterns of patients in this bone oncology investigation. GCTB was seen in 85.9 % of positive cases, primarily round in form (55.5 %), and typically displayed a multifocal, peripheral, and multilobar distribution. These findings are consistent with those reported by Salehi et al. [21], who found GCTB in 88 % of the 919 patients in their study. Similarly, Ojha et al. [22] analyzed 45 studies involving 4410 adult patients and reported solo GCTB in 50.2 % of cases and mixed GCTB with osteolytic lesions in 44.4 % of cases. Other studies have reported even higher incidences of GCTB, emphasizing its significance in bone cancer diagnostics [23]. The multifocal, peripheral, and multilobar distribution of GCTB emerged as the most specific criteria for detecting bone cancer, with the highest incidence noted in multiple studies [24].

The trabecular disorganization pattern was the second most frequent imaging feature, observed in 45.3 % of individuals. Following this, the periosteal reaction sign was noted in 29.4 % of positive cases. Ojha et al. [22] reported periosteal reaction in 64 % of cases, while describing the trabecular disorganization pattern in 19.5 % of positive cases. Li et al. [23] identified the trabecular disorganization pattern in 36 % of cases, and Bai et al. [25] found periosteal reaction signs in 59 % of bone cancer patients. Consolidation, indicating the replacement of normal bone marrow with pathological tissue, can reflect disease severity and progression [26]. Studies show varying frequencies of bone consolidation in imaging of new bone cancer cases, ranging from 2 % to 64 % [8]. In the current study, 28.8 % of confirmed cases exhibited consolidation, with a notably higher rate (81.5 %) among patients admitted to the ICU. Additionally, consolidation was the predominant imaging feature in 66.7 % of ICU cases. These findings suggest two distinct imaging phenotypes in bone cancer: one dominated by consolidation and the other by GCTB. Significantly, the phenotype characterized by predominant consolidation appears to correlate with poorer prognosis, indicating a higher likelihood of adverse outcomes.

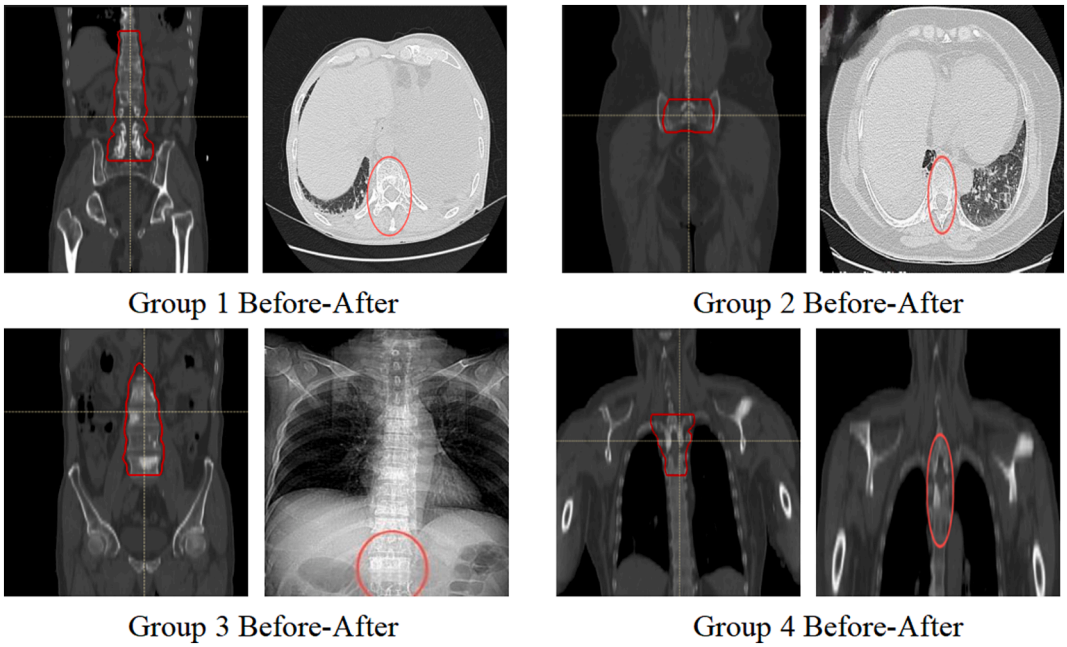


**Fig. 2.** CT scans from medical records of groups 1 to 4 before and after the nursing period.

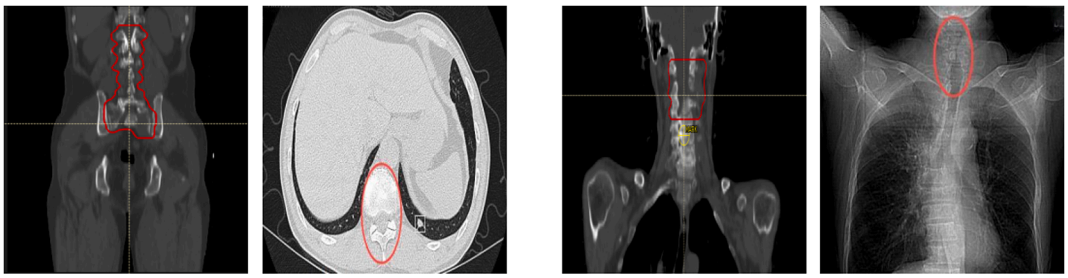


**Fig. 3.** Analyzing CT scans from medical records of groups 5–6 both before and after the study period.

**Table 2**
Age of the Research Group Compared to CT Severity Score and Consolidation Pattern in Bone Cancer and Oncology Patients.

| Variables | | ≤ 18.0 (N = 39) | 19.0–59.0 (N = 340) | ≥ 60.0 (N = 87) | P value |
|---|---|---|---|---|---|
| **Normal healthy** | | 13 (33.3 %) | 76 (22.4 %) | 39 (44.8 %) | # **<0.001** * |
| **Abnormal GCTB** | | 12 (30.8 %) | 38 (11.2 %) | 27 (31.0 %) | # **<0.001** * |
| **Consolidation location** | **Lobar** | 8 (61.5 %) | 17 (22.4 %) | 17 (43.6 %) | # **0.005*** |
| | **Sub- and segmental** | 5 (38.5 %) | 59 (77.6 %) | 22 (56.4 %) | |
| **Clinical seriousness** | **ICU** | 2 (18.2 %) | 30 (11.3 %) | 22 (34.9 %) | # < **0.001*** |
| | **Hospital** | 1 (9.1 %) | 47 (17.7 %) | 22 (34.9 %) | |
| | **Home** | 8 (72.7 %) | 189 (71.1 %) | 19 (30.2 %) | |

## 4. Discussion

In response to the increasing number of patients suspected of having bone cancer and the variability in diagnostic test results, this study investigated the utility of imaging modalities, including computed tomography (CT), to enhance diagnostic accuracy and clinical decision-making. The study focused on the use of CT scans to supplement clinical and laboratory findings in diagnosing bone cancer. Strict infection control [44] measures, following guidelines from the Fleischer Society, were implemented to prevent transmission. Specifically, one dedicated CT scanner was allocated for screening suspected bone cancer patients, while routine medical services continued to be provided using other scanners. This approach aimed to optimize diagnostic efficiency and patient management strategies amidst diagnostic challenges.

The results of this study revealed that CT imaging had a 92.6 % sensitivity in identifying bone cancer [13]. However, this sensitivity was lower than the 97 % to 98 % observed in earlier investigations [11,16]. This discrepancy may be partially attributed to the 7.4 % of our positive cases with normal CT scans, conducted too soon after symptom onset (two to three days). It has been reported that within 0–2 days after the onset of symptoms, 50 % of patients had normal CT scans [19]. In 69.7 % of positive cases, high-likelihood CT criteria were met, adhering to the highest recommendations from the Radiological Society of North America (RSNA). These cases also exhibited the highest positive predictive value (PPV) (98.8 %) and specificity (97.6 %) [18], and found that 72 % of patients had normal CT findings. Additionally, 7.4 % of positive cases had a negative CT pattern, suggesting that a negative CT should not be the sole criterion for ruling out bone cancer, contrary to ACR guidelines [20]. The specificity of CT probability, as determined by RSNA guidelines, was higher in the high probability group (97.6 %) and gradually declined in the low probability group (67.5 %) [20]. This suggests an increasing number of true positive cases among patients with high CT probability.

Giant Cell Tumor of Bone (GCTB) was the most common feature observed in the imaging patterns of patients in this bone oncology investigation. GCTB was seen in 85.9 % of positive cases, primarily round in form (55.5 %), and typically displayed a multifocal, peripheral, and multilobar distribution. These findings are consistent with those reported [21], who found GCTB in 88 % of the 919 patients in their study. Similarly, One particular study [22] analyzed 45 studies involving 4410 adult patients and reported solo GCTB in 50.2 % of cases and mixed GCTB with osteolytic lesions in 44.4 % of cases. Other studies have reported even higher incidences of GCTB, emphasizing its significance in bone cancer diagnostics [23]. The multifocal, peripheral, and multilobar distribution of GCTB emerged as the most specific criteria for detecting bone cancer, with the highest incidence noted in multiple studies [24].

The trabecular disorganization pattern was the second most frequent imaging feature, observed in 45.3 % of individuals. Following this, the periosteal reaction sign was noted in 29.4 % of positive cases. It has been reported periosteal reaction in 64 % of cases, while describing the trabecular disorganization pattern in 19.5 % of positive cases [22]. It has also been identified the trabecular disorganization pattern in 36 % of cases, and found periosteal reaction signs in 59 % of bone cancer patients [23,25]. Consolidation, indicating the replacement of normal bone marrow with pathological tissue, can reflect disease severity and progression [26]. Studies show varying frequencies of bone consolidation in imaging of new bone cancer cases, ranging from 2 % to 64 % [8]. In the current study, 28.8 % of confirmed cases exhibited consolidation, with a notably higher rate (81.5 %) among patients admitted to the ICU. Additionally, consolidation was the predominant imaging feature in 66.7 % of ICU cases. These findings suggest two distinct imaging phenotypes in bone cancer: one dominated by consolidation and the other by GCTB. Significantly, the phenotype characterized by predominant consolidation appears to correlate with poorer prognosis, indicating a higher likelihood of adverse outcomes.

Our study demonstrated a strong correlation between patient management decisions and CT severity scores. A score of less than 10 suggested home isolation, while scores above 14 indicated ICU hospitalization. It has been found a CT severity score cutoff of 19.5 out of 40 to predict severe cases with 83.3 % sensitivity and 94 % specificity [36]. Future implementations could enhance CT image analysis and ICU need forecasts using neural network [45] algorithms and optimization techniques [38–41].

Fig. 4 depicts the distribution of consolidation locations ('Lobar' and 'Sub- and segmental') across various clinical seriousness categories (ICU, Hospital, Home) within the cohort of bone cancer and oncology

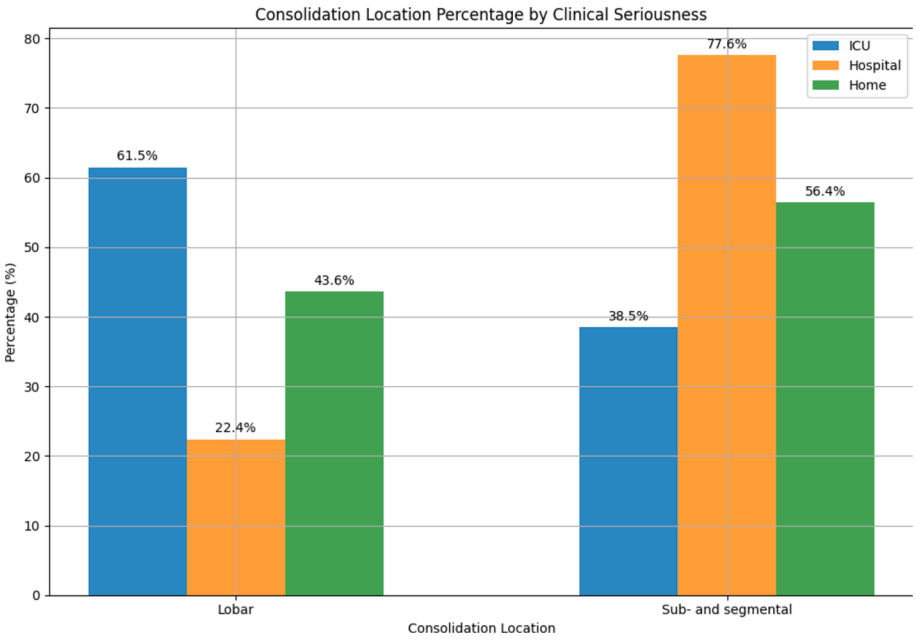


**Fig. 4.** Distribution of consolidation locations ('Lobar' and 'Sub- and segmental') across clinical seriousness categories (ICU, Hospital, Home) in bone cancer and oncology patients.

patients studied. It highlights distinct patterns of consolidation localization based on the severity of clinical presentation. In the ICU setting, 'Lobar' consolidation is prominently observed, accounting for 61.5 % of cases, whereas 'Sub- and segmental' consolidation represents 38.5 %. This indicates a preference for more centralized or extensive healthcare involvement in critically ill patients. In contrast, in the Hospital setting, 'Sub- and segmental' consolidation predominates with 77.6 %, suggesting a broader distribution of bone tumors. Patients managed at home show a more balanced distribution, with 'Lobar' consolidation at 43.6 % and 'Sub- and segmental' consolidation at 56.4 %. Variability is quantitative measurements is a common phenomenon in real life, and the patterns of variation can often be analysed [46–48]. Our findings underscore the variability in consolidation patterns based on the clinical context, providing insights that could influence treatment strategies and [30] prognostic assessments in bone cancer and oncology patients. For future implementations, machine learning [49–51] and other state of the art optimization techniques [52–54], as well as 3D visualization technology [55–57] can be utilized to improve health diagnostics to a more advanced level.

## 5. Conclusion

Computed tomography (CT) has emerged as a valuable method for the prompt and accurate identification and management of bone cancer. It facilitates early disease detection and intervention, enabling timely treatment measures to improve patient outcomes. Our study underscores the efficacy of using established radiological criteria in reporting suspected bone cancer cases, particularly given that negative CT scan results may occur early in the disease course. To minimize false-negative results, a CT examination is recommended at strategic intervals after initial symptom presentation. The two primary CT features associated with bone cancer are Giant Cell Tumor of Bone (GCTB) and consolidation patterns, with the latter being notably significant in advanced stages of the disease. The presence of a consolidation pattern indicates more aggressive disease and may necessitate more intensive treatment protocols. Additionally, CT severity scores are instrumental in predicting both the need for aggressive treatment and the extent of bone involvement. These findings highlight the critical role of CT imaging in guiding clinical decision-making and optimizing patient management in bone cancer and other oncology cases where rapid and accurate diagnosis is essential.

## 6. Ethics approval and consent to participate

This study received approval from the institutional board of ethics.

## 7. Consent for publication

Yes.

## CRediT authorship contribution statement

**Huan Xu:** Writing – review & editing, Writing – original draft. **Qunfang Zhao:** Data curation. **Xiaoyan Miao:** Data curation. **Lijun Zhu:** Software. **Junping Wang:** Methodology.

## Declaration of competing interest

The authors declare that they have no known competing financial interests or personal relationships that could have appeared to influence the work reported in this paper.

## References

[1] A. Ratley, J. Minj, and P. Patre, "Leukemia disease detection and classification using machine learning approaches: A review,'' in Proc. 1st Int. Conf. Power, Control Comput. Technol. (ICPC2T), Jan. 2020, pp. 161–165.
[2] M. W. Nadeem, H. G. Goh, A. Ali, M. Hussain, M. A. Khan, and V. A. P. Ponnusamy, "Bone age assessment empowered with deep learning: A survey, open research challenges and future directions,'' Diagnostics,.
[3] V.O. Lewis, M.T. Deavers, P.P. Lin, et al., Huvos AG. Bone Sarcoma, in: Bone and Soft Tissue Pathology, 1st ed., Elsevier, Philadelphia, 2008, pp. 299–325.
[4] Jaffe N, Bruland OS, Bielack SS (2011) Pediatric and Adolescent Osteosarcoma. Springer Science & Business Media. ISBN: 978-1-4419-6101-3.
[5] Bielack SS, Carrle D, Hardes J, et al. (2008) Bone Tumors: Osteosarcoma, Ewing's Sarcoma, and Chondrosarcoma. In: Pediatric Hematology/Oncology. Springer. p. 541-584. DOI: 10.1007/978-3-540-74142-8_30.
[6] M. Herrera-Perez, L. Guerrero, J. De La Maza, et al., Bone sarcoma in adults: Outcome after multimodal treatment, J. Surg. Oncol. 120 (7) (2019) 1288–1297, https://doi.org/10.1002/jso.25630.
[7] K. Cheung, Y. Wang, W. Chow, et al., Functional outcomes after limb salvage and reconstruction using an extendable prosthesis for pediatric osteosarcoma around

the knee, Bone Joint J 100-B(4) (2018) 484–492, https://doi.org/10.1302/0301-620X.100B4.BJJ-2017-0764.R1.
[8] A. Freeman, G. Kwan-Lim, D. Shaw, et al., Myxoid liposarcoma with extensive high-grade areas. A morphologic and immunohistochemical study of 11 cases, Am. J. Surg. Pathol. 33 (10) (2009) 1472–1479, https://doi.org/10.1097/PAS.0b013e3181b13f7a.
[9] G. Markhede, B. Stener, A. Rydholm, Surgical treatment of chondrosarcoma, Acta Orthop. Scand. 52 (5) (1981) 567–574, https://doi.org/10.3109/17453678108992184.
[10] T. Heare, M.A. Hensley, S. Dell'Orfano, Bone tumors: Osteosarcoma and Ewing's sarcoma, Curr. Opin. Pediatr. 21 (3) (2009) 365–372, https://doi.org/10.1097/MOP.0b013e32832b111e.
[11] F.J. Hornicek, M.C. Gebhardt, N. Duval-Couetil, et al., Allograft reconstruction of the shoulder after bone tumor resection, Clin. Orthop. Relat. Res. 426 (2004) 44–50, https://doi.org/10.1097/01.blo.0000131548.57376.fd.
[12] P.A. Meyers, R. Gorlick, Osteosarcoma, Pediatr. Clin. North Am. 44 (4) (1997) 973–989, https://doi.org/10.1016/S0031-3955(05)70536-6.
[13] N. Marina, M. Gebhardt, L. Teot, et al., Biology and therapeutic advances for pediatric osteosarcoma, Oncologist 9 (4) (2004) 422–441, https://doi.org/10.1634/theoncologist.9-4-422.
[14] P.C. Ferguson, B.M. Deheshi, P. Chung, et al., Soft tissue sarcoma presenting with metastatic disease: Outcome with primary surgical resection, Cancer 115 (5) (2009) 1048–1054, https://doi.org/10.1002/cncr.24118.
[15] G. Rosen, M.L. Murphy, A.G. Huvos, et al., Chemotherapy, en bloc resection, and prosthetic bone replacement in the treatment of osteogenic sarcoma, Cancer 41 (3) (1978) 1431–1437, https://doi.org/10.1002/1097-0142(197803)41:3<1431::AID-CNCR2820410338>3.0.CO;2-J.
[16] J. Bickels, J.C. Wittig, Y. Kollender, et al., Distal femur resection with endoprosthetic reconstruction: A long-term followup study, Clin. Orthop. Relat. Res. 400 (2002) 225–235, https://doi.org/10.1097/00003086-200207000-00028.
[17] G. Scoccianti, F. Frenos, C. Greco, et al., Custom 3D-printed prosthetic reconstructions: feasibility, safety and indications. A systematic review of the literature and a presentation of a series of 14 patients, Orthop. Traumatol. Surg. Res. 104 (8) (2018) 1239–1246, https://doi.org/10.1016/j.otsr.2018.07.011.
[18] C.D.M. Fletcher, J.A. Bridge, P.C.W. Hogendoorn, et al., WHO Classification of Tumours of Soft Tissue and Bone, 4th ed., IARC Press, Lyon, 2013.
[19] H.D. Dorfman, B. Czerniak, Bone cancers, Cancer 75 (1 Suppl) (1995) 203–210, https://doi.org/10.1002/1097-0142(19950101)75:1+<203::AID-CNCR2820751318>3.0.CO;2-X.
[20] S. Boriani, A. Gasbarrini, S. Bandiera, et al., En bloc resections of bone tumors of the thoracolumbar spine: A consecutive series of 20 patients treated by the same team, Spine 31 (26) (2006) 325–334, https://doi.org/10.1097/01.brs.0000251271.15711.e1.
[21] I.C. Dickinson, D.J. Whitwell, J.J. Battista, et al., Surgical treatment of chondrosarcoma, Cancer 88 (3) (2000) 640–647, https://doi.org/10.1002/(SICI)1097-0142(20000201)88:3<640::AID-CNCR26>3.0.CO;2-T.
[22] S.S. Bielack, B. Kempf-Bielack, G. Delling, et al., Prognostic factors in high-grade osteosarcoma of the extremities or trunk: An analysis of 1,702 patients treated on neoadjuvant cooperative osteosarcoma study group protocols, J. Clin. Oncol. 20 (3) (2002) 776–790, https://doi.org/10.1200/JCO.20.3.776.
[23] G. Bacci, S. Ferrari, S. Lari, et al., Osteosarcoma of the limb. Amputation or limb salvage in patients treated by neoadjuvant chemotherapy, J. Bone Joint Surg. Br. 84 (1) (2002) 88–92, https://doi.org/10.1302/0301-620X.84B1.0840088.
[24] M.S. Kim, S.Y. Lee, W.H. Cho, et al., An analysis of the accuracy of magnetic resonance imaging and computed tomography for detecting the intraosseous extent of bone sarcomas, J. Bone Joint Surg. Am. 94 (12) (2012) e87.
[25] E.A. Levine, M.T. Scarborough, Stage IA extremity soft tissue sarcoma: Long-term outcome and prognostic factors, Sarcoma 6 (2) (2002) 59–65, https://doi.org/10.1080/13577140220127848.
[26] P.C. Hogendoorn, N. Athanasou, S. Bielack, et al., Bone sarcomas: ESMO Clinical Practice Guidelines for diagnosis, treatment, and follow-up, Ann. Oncol. 21 (Suppl 5) (2010) v204–v213, https://doi.org/10.1093/annonc/mdq223.
[27] R.T. Ellati, D.M. Lindskog, R.K. Munn, et al., Prognostic factors and survival in chondrosarcoma: An analysis of 156 patients with complete long-term follow-up, Orthopedics 36 (3) (2013) e271–e276, https://doi.org/10.3928/01477447-20130222-12.
[28] Bone Tumour Committee of the Japanese Orthopaedic Association, Histological typing of bone tumours, Springer-Verlag, Berlin Heidelberg, 2012.
[29] A.S. Pappo, M. Devidas, J. Jenkins, et al., Risk-adapted chemotherapy for young children with newly diagnosed extraosseous Ewing sarcoma: A Children's Oncology Group phase III trial, J. Clin.oncol 25 (8) (2007) 914–920, https://doi.org/10.1200/JCO.2006.08.5172.
[30] K. Song, J. Song, H. Kang, et al., Prognostic factors and clinical outcomes of patients with high-grade extremity osteosarcoma without complete surgical remission, J Bone Oncol 13 (2018) 17–21, https://doi.org/10.1016/j.jbo.2018.10.001.
[31] S. Tokunaga, A. Sakai, H. Yamada, et al., Long-term outcome of patients with high-grade osteosarcoma: a single-institution experience, Anticancer Res 39 (2) (2019) 899–904, https://doi.org/10.21873/anticanres.13206.
[32] Y. Li, Y. Cai, H. Li, et al., Prognostic significance of systemic immune-inflammation index in patients with osteosarcoma, Clin. Chim. Acta 502 (2020) 239–244, https://doi.org/10.1016/j.cca.2019.12.024.
[33] P.A. Meyers, C.L. Schwartz, M.D. Krailo, et al., Osteosarcoma: The addition of muramyl tripeptide to chemotherapy improves overall survival–a report from the Children's Oncology Group, J. Clin. Oncol. 26 (4) (2008) 633–638, https://doi.org/10.1200/JCO.2008.14.0095.
[34] H. Gelderblom, R.C. Jinks, M.R. Sydes, et al., Survival outcomes from a randomized comparison of two doses of mifamurtide (L-MTP-PE) in combination with postoperative chemotherapy for patients with resectable osteosarcoma, Eur. J. Cancer 84 (2017) 130–138, https://doi.org/10.1016/j.ejca.2017.07.012.
[35] J.L. Beebe-Dimmer, K. Cetin, J.P. Fryzek, et al., The epidemiology of malignant giant cell tumors of bone: an analysis of data from the Surveillance, Epidemiology and End Results Program (1975–2004), Rare Tumors 1 (2) (2005) e52.
[36] H.S. Schwartz, J.M. Cates, Evidence-based pathologic parameters for prognostication in osteosarcoma, Ann. Diagn. Pathol. 10 (6) (2006) 427–438, https://doi.org/10.1016/j.anndiagpath.2006.05.003.
[37] C.D.M. Fletcher, J.A. Bridge, P.C.W. Hogendoorn, F. Mertens (Eds.), WHO Classification of Tumours of Soft Tissue and Bone, 4th ed., IARC Press, Lyon, 2013.
[38] R. Yang, X. Li, H. Liu, et al., Prognostic significance of skeletal-related events for overall survival in patients with bone metastasis from lung cancer, J. Cancer Res. Clin. Oncol. 145 (3) (2019) 737–746, https://doi.org/10.1007/s00432-018-02834-6.
[39] L. Xu, Z. Zhao, X. Shang, et al., Identification of differentially expressed genes and biological pathways in osteosarcoma by integrated analysis of multiple gene expression datasets, Sci. Rep. 9 (1) (2019) 12488, https://doi.org/10.1038/s41598-019-48966-w.
[40] L. Kager, A. Zoubek, U. Pötschger, et al., Primary metastatic osteosarcoma: Presentation and outcome of patients treated on neoadjuvant Cooperative Osteosarcoma Study Group protocols, J. Clin. Oncol. 21 (10) (2003) 2011–2018, https://doi.org/10.1200/JCO.2003.08.132.
[41] P.G. Casali, S. Bielack, N. Abecassis, et al., Bone sarcomas: ESMO–EURACAN Clinical Practice Guidelines for diagnosis, treatment and follow-up, Ann. Oncol. 29 (Suppl 4) (2018) iv79-iv95, https://doi.org/10.1093/annonc/mdy310.
[42] Y. Zhou, X. Duan, X. Zhang, et al., Prognostic factors for survival in patients with primary malignant bone tumors: A large retrospective study, Ann Transl Med 8 (4) (2020) 822, https://doi.org/10.21037/atm-20-1311.
[43] T.F. DeLaney, L. Park, S.I. Goldberg, et al., Radiotherapy for local control of osteosarcoma, Int. J. Radiat. Oncol. Biol. Phys. 76 (4) (2010) 1147–1153, https://doi.org/10.1016/j.ijrobp.2009.03.013.
[44] T. Zhenhao, S. Mengxuan, Xu. Wang, X. Wenyuan, Y. Yuan, W. Zhi, O. Tinghui, Theory-guided Deep Neural Network for boiler 3-D NOx concentration distribution prediction, Energy 2024 (2024) 131500, https://doi.org/10.1016/j.energy.2024.131500.
[45] M. Liu, J. Lv, S. Du, Y. Deng, X. Shen, Y. Zhou, Multi-resource constrained flexible job shop scheduling problem with fixture-pallet combinatorial optimisation, Comput. Ind. Eng. 188 (2024) 109903.
[46] Delin Huang, Shichang Du, Guilong Li, and Zhuoqi Wu. A systematic approach for on-line minimizing volume difference of multiple chambers in machining processes based on high definition metrology. ASME Transaction on Manufacturing Science and Engineering. 2017. 139(8): 081003-1-17.
[47] Shichang Du and Lan Fei. Co-Kriging method for form error estimation incorporating condition variable measurements. ASME Transaction on Journal of Manufacturing Science and Engineering. 2016.138, 041003-1-16.
[48] G. Li, Du. Shichang, Elastic mechanics-based fixturing scheme optimization of variable stiffness structure workpieces for surface quality improvement, Precis. Eng. 56 (2019) 343–363.
[49] X. Xue, W. Chen, X. Chen, A Novel Radiomics-Based Machine Learning Framework for Prediction of Acute Kidney Injury-Related Delirium in Patients Who Underwent Cardiovascular Surgery, Comput. Math. Methods Med. 2022 (1) (2022) 4242069.
[50] X. Xue, Z. Liu, T. Xue, W. Chen, X. Chen, Machine learning for the prediction of acute kidney injury in patients after cardiac surgery, Front. Surg. 2022 (9) (2022) 946610.
[51] Z. Tang, S. Wang, Y. Li, Dynamic NOX emission concentration prediction based on the combined feature selection algorithm and deep neural network, Energy 2024 (292) (2024) 130608, https://doi.org/10.1016/j.energy.2024.130608.
[52] Du. Shichang, Xu. Rui, L. Li, Modeling and Analysis of Multiproduct Multistage Manufacturing System for Quality Improvement, IEEE Transaction on Systems, Man, and Cybernetics: Systems. 48 (5) (2018) 801–820.
[53] Guilong Li, Shichang Du, Bo Wang, Jun Lv, Yafei Deng. High Definition Metrology-Based Quality Improvement of Surface Texture in Face Milling of Workpieces with Discontinuous Surfaces. ASME Transaction on Manufacturing Science and Engineering. 2022, 144: 031001-1-18.
[54] Guilong Li, Shichang Du, Delin Huang, Chen Zhao, Yafei Deng, Dynamics Modeling-Based Optimization of Process Parameters in Face Milling of Workpieces with Discontinuous Surfaces, ASME Transaction on Manufacturing Science and Engineering. 2019. 141: 101009-1-15.
[55] C. Zhao, J. Lv, Du. Shichang, Geometrical Deviation Modeling and Monitoring of 3D Surface Based on Multi-output Gaussian Process, Measurement 199 (2022) 111569.
[56] S.C.P. Cheung, K.K.L. Wong, W. Yang, G.H. Yeoh, J.Y. Tu, R. Beare, T. Phan, Experimental and numerical study on the hemodynamics of stenosed carotid bifurcation, Australas. Phys. Eng. Sci. Med. 33 (4) (2010) 319–328.
[57] Y. Shao, Y. Yin, Du. Shichang, T. Xia, L. Xi, Leakage Monitoring in Static Sealing Interface Based on Three Dimensional Surface Topography Indicator, ASME Trans. Manuf. Sci. Eng. 140 (10) (2018) 101003.